JACS Hosting Innovations

Contents List available at JACS Directory

# **Journal of Advanced Chemical Sciences**

journal homepage: www.jacsdirectory.com/jacs



## Bifurcation Structures of the Classical Morse Oscillator under the Excitation of Different Periodic Forces

S. Guruparan<sup>1</sup>, B. Ravindran Durai Nayagam<sup>2</sup>, S. Selvaraj<sup>3</sup>, V. Ravichandran<sup>4</sup>, V. Chinnathambi<sup>4,\*</sup>

#### ARTICLEDETAILS

Article history:
Received 02 November 2015
Accepted 11 November 2015
Available online 16 November 2015

Keywords:
Morse Oscillator
Periodic Forces
Bifurcations
Chaos
Period-Bubble Orbit

#### ABSTRACT

Bifurcation structures of the classical Morse oscillator with different shapes of periodic forces are studied numerically in detail. The external periodic forces considered in our study are sine wave, square wave, symmetric and asymmetric saw tooth waves, rectified sine wave and modulus of sine wave. Transcritical bifurcation, period doubling bifurcation, chaos, intermittency, periodic windows, reverse period doubling bifurcation, period-3 bubble orbit are found to occur due to the applied forces. Numerical results are demonstrated through bifurcation diagram, phase portrait and Poincare map. A comparative study of various forces is also performed.

## 1. Introduction

The driven Morse oscillator is a standard model frequently used in theoretical chemistry for describing many molecular phenomena, such as interaction of a molecule with electromagnetic radiation [1-5]. In recent years, many researchers studied the dynamics of Morse oscillator with classical, semiclassical and quantum mechanical methods [6-12]. In particular Lie et al. [13] numerically studied the bistable and chaotic behavior in a damped driven Morse oscillator by solving a classical equation. Knob et al. [14] investigated the bifurcation structure of the classical Morse oscillator using bifurcation diagram, fixed-point diagram and phase portraits. Parthasarathy et al. [15] investigated the analytic structure of the solution of damped and driven Morse oscillator is carried out after effecting an exponential transformation. Rong-Wei et al. [16] studied the dynamics of the driven Morse oscillator qualitatively by analytic methods. Jing et al. [17] investigated the bifurcations of periodic orbits and chaos in damped and driven Morse oscillator by both analytically and numerically. Heagy et al. [18] studied the classical dynamics of one dimensional Morse oscillator subjected to periodic impulsive (delta function) force. Behnia et al. [19] have investigated the controlling chaos in a damped and driven Morse oscillator via slavemaster feedback. Gan et al. [20] analysed the process of torus breakdown transforming the original system into another one in action-angle variables. In classical Morse oscillator, Kapral et al. [21] have found perioddoubling, tangent bifurcations, chaos using Poincare maps, bifurcation diagrams and amplitude resonance curves. Beigie et al. [22] investigated the chaotic dynamics associated with a quasiperiodically forced Morse oscillator using Melnikov method. In a very recent paper, Zhou et al. [23] studied both analytically and numerically the chaotic motion of a damped and driven Morse oscillator and Abirami et al. [24] investigated the occurrence of vibrational resonance in classical and quantum mechanical Morse oscillator driven by biharmonic force.

Motivated by the above, in the present paper, we wish to investigate the bifurcation structures of the classical Morse oscillator subjected to

$$\ddot{x} + d\dot{x} + \beta e^{-\alpha x} (1 - e^{-\alpha x}) = F(t), \tag{1}$$

where  $\beta$  and  $\alpha$  are the dissociation energy and the Morse spectroscopic term or the range parameter, respectively, d and F(t) are the velocity proportional damping parameter and the external forcing term respectively. In the absence of external forcing and damping terms (ie. F(t)=0 and d=0) the potential of the Morse oscillator is given by [1-3].

$$V(x) = \frac{1}{2\alpha} \beta e^{-\alpha x} (e^{-\alpha x} - 2)$$

Fig. 1 depicts the form of the Morse potential (solid line) and harmonic potential (dotted line). The Morse potential realistically leads to dissociation, making it more useful than the harmonic potential. The Morse potential is the simplest representative of the potential between two nuclei in which dissociation is possible. For over the past three decades, the Morse potential have provided a useful model for the interatomic potential and for fitting the vibrational spectra of diatomic molecules [1, 2].

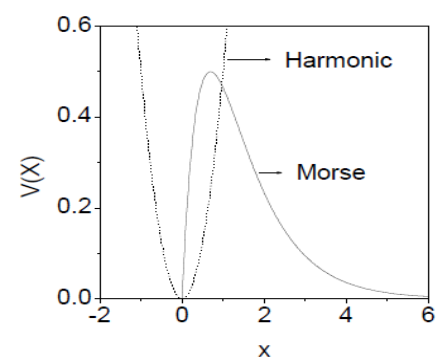


Fig. 1 Morse potential curve for  $\beta$  = 2.0 and  $\alpha$  = 1 (solid line). Harmonic potential curve (dotted curve ).

<sup>&</sup>lt;sup>1</sup>Department of Chemistry, Sri K.G.S Arts College, Srivaikuntam – 628619, Tamilnadu, India.

<sup>&</sup>lt;sup>2</sup>Department of Chemistry, Pope's College, Sawyerpuram – 628251, Tamilnadu, India.

<sup>&</sup>lt;sup>3</sup>Department of Physics, The M.D.T. Hindu College, Tirunelveli – 627012, Tamilnadu, India.

<sup>&</sup>lt;sup>4</sup>Department of Physics, Sri K.G.S Arts College, Srivaikuntam – 628619, Tamilnadu, India.

different periodic forces. The equation of motion of damped and driven classical Morse oscillator equation is

<sup>\*</sup>Corresponding Author

Email Address: veerchinnathambi@gmail.com (V. Chinnathambi)

At present the Morse oscillator is commonly used for diatomic. The damped and driven Morse oscillator (Eq. 1) can serve as a rough model for the following problems [25-29]:

- Multiphoton excitation and dissociation of diatomic molecules in a dense medium or in a gaseous cell under high pressure.
- (ii) Pumping of a local mode of a polyatomic molecule by an infrared laser; where the energy flow out of the molecule (by mode-mode coupling, collisions etc.) is modeled by a single decay constant.
- (iii) The anamolous gains observed in stimulated Raman emission and
- (iv) The dissociation of vander waal complexes.

## 2. Types of Periodic Forces

The external periodic forces of our interest are (i) sine wave, (ii) square wave, (iii) symmetric saw tooth wave, (iv) asymmetric saw tooth wave, (v) rectified sine wave and (vi) modulus of sine wave. The period-T of all the forces considered in our study is fixed as  $2\pi/\omega$ . Mathematical forms of periodic force are the following.

$$F_{\sin}(t) = F_{\sin}(t + 2\pi/\omega) = f \sin \omega t, \tag{3}$$

$$F_{sq}(t) = F_{sq}(t + 2\pi/\omega) = fsqn(\sin \omega t), \tag{4}$$

$$F_{rec}(t) = F_{rec}(t + 2\pi/\omega) = \begin{cases} f \sin \omega t, & 0 < t < \pi/\omega \\ 0, & \pi/\omega < t < 2\pi/\omega, \end{cases}$$
 (5)

$$F_{sst}(t) = F_{sst}(t + 2\pi/\omega) = \begin{cases} 4ft/T, & 0 < t < \pi/\omega \\ -4ft/T + 2f, & \pi/2\omega < t < 3\pi/2\omega \\ 4ft/T - 4f, & 3\pi/2\omega < t < 2\pi/\omega, \end{cases}$$
(6)

$$F_{ast}(t) = F_{ast}(t + 2\pi/\omega) = \begin{cases} 2ft/T, & 0 < t < \pi/\omega \\ 2ft/T - 2f, & \pi/\omega < t < 2\pi/\omega, \end{cases}$$
 (7)

$$F_{msi}(t) = F_{msi}(t + 2\pi/\omega) = f \left| \sin \omega t / 2 \right|. \tag{8}$$

Where sqn(y) is sign y,  $T = 2\pi/\omega$  and is taken as mod(T). When the system (Eq.1) is subjected to external periodic force, the potential has an additional term – x F(t).

# 3. Analysis of Bifurcation Structures due to the Applied Periodic Forces

For our numerical calculation we transform the second order differential equation (Eq. 1) into an autonomous system of first order differential equation of the following form

$$\dot{x} = y, \tag{9a}$$

$$\dot{y} = -dy - \beta e^{-\alpha x} (1 - e^{-\alpha x}) + F(t).$$
 (9b)

For our numerical study we fix d=0.8,  $\beta=8.0$ ,  $\alpha=1$  and  $\omega=2$ . Eq. 9 is solved with different periodic forces by Runge-Kutta fourth order method with time step size  $2\pi/\omega/200$ . Numerical solution corresponding to 500 drive cycle is left as transient. We analyzed the response of the system (Eq. 9) by varying the forcing amplitude of each periodic forces.

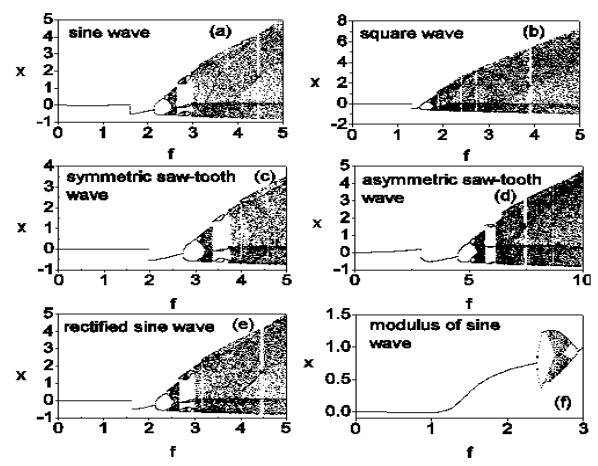
## 3.1 Transcritical Bifurcation

Fig. 2 shows the bifurcation structures for various forces. We can clearly notice many similarities and differences in the bifurcation pattern when the control parameter f is varied. Consider the effect of the force  $f\sin\omega t$  at  $f_{\sin} = f_{\sin,t} = 1.60794$ , a transcritrical bifurcation occurs at which the maximal Lyapunov exponent  $(\lambda_m) \approx 0$ . When the force  $f\sin\omega t$  is replaced by other forces similar behavior is found. The values of forcing amplitude of different forces at which transcritical bifurcation observed are  $f_{sq,t} = 1.30984$ ,  $f_{rec,t} = 1.62150$ ,  $f_{ss,t} = 1.99083$ ,  $f_{ast,t} = 2.92987$  and  $f_{ms,t} = 1.20529$ . That is the bifurcation occurs relatively earlier in the case of modulus of sine wave force whereas it is very much delayed in asymmetric saw tooth wave force. Fig. 3 shows the phase portraits for few values of f for various forces. For small values of f of certain forces the orbits have cusp-like structure due to the discontinuity in the applied forces.

## 3.2 Period Doubling and Chaos

When the value of the forcing amplitude is increased from transcritical bifurcation a period doubling phenomenon leading to chaotic motion is realized for all the forms of forces. This is shown in Fig. 2. In Fig. 2a with the force being f sin  $\omega$ t at  $f_{\sin}$  = 2.13431 the period-T orbit becomes unstable and a period-2T orbit is born. Bifurcation to period 4T, 8T and

16T orbits are found to occur at  $f_{sin} = 2.37859$ , 2.4401 and 2.4511 respectively. The period doubling sequence accumulated at  $f_{sin}$  = 2.4556. At this value of  $f_{sin}$  onset of chaos is observed. When the external force is square wave, the period 2T, 4T, 8T and 16T orbit bifurcations occurred at  $f_{sq} = 1.6665$ , 1.71744, 1.72648 and 1.72875 respectively. The critical values of f at which various bifurcations occur for different forms of forces are summarized in Table 1. From the Table 1 and the Fig. 2, we note that when f is increased from a small value, period doubling phenomenon is realized much earlier for square wave, while it is relatively at a higher value of f for the asymmetric saw-tooth wave. For all the forces we studied the behaviour in the interval  $f \in [0,10]$  As the value of forcing amplitude is increased beyond the onset of chaos, bifurcations of chaos such as band merging and sudden widening of a chaotic attractor, intermittency, period-3 bubble orbit and reverse period doubling bifurcation are observed for all the forces. However the bifurcations occurred at different values of forcing amplitude. Chaotic regions of interval of f are small for the modulus of sine wave. This is clearly evident in Fig. 2. Fig. 4 shows phase portraits at the accumulation of period doubling phenomenon (onset of chaos) for various forces. The geometrical structure of the attractor is different for various forces. Cross-well chaotic motion is formed for all the forces except for modulus of sine wave force. Period-3 bubble orbit occurs for all the forces except square wave and modulus of sine wave forces which are clearly shown in Fig. 5. For modulus of sine wave force, the system (Eq. 9) starts with period doubling followed by chaotic motion and reverse-period doubling bifurcation. This is clearly evident in Fig. 2. The Poincare map of the chaotic attractor of the system (Eq. 9) for various forces is shown in Fig. 6. It has been drawn using points collected at  $2\pi/\omega$  time intervals, that is, at every period of the external periodic force of the system (Eq. 9). The geometrical structure of the chaotic attractor in the Poincare map appears as a totally disconnected at uncountable set of points.



**Fig. 2** Bifurcation structures of classical Morse oscillator (Eq.9) driven by different periodic forces. The values of other parameters are d = 0.8,  $\beta = 8.0$ ,  $\alpha = 1$  and  $\omega = 2$ .

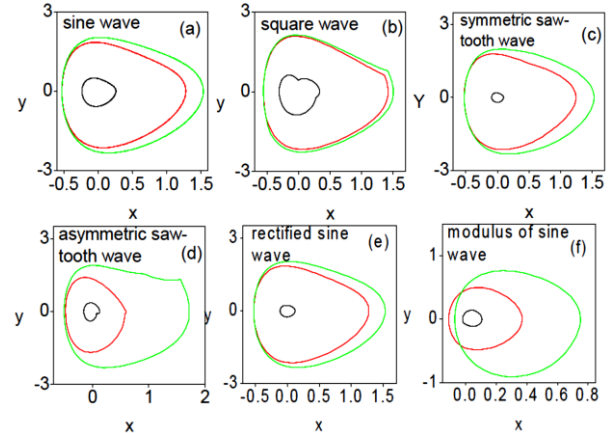


**Fig. 3** Phase portraits of the system (Eq.9) near transcritical bifurcation for various forces. The values of other parameters are d = 0.8,  $\beta = 8.0$ ,  $\alpha = 1$  and  $\omega = 2$ .

### 3.3 Intermittency Transitions

Next we show the occurrence of intermittency transition to chaos in the system (Eq. 1) driven by periodic sine wave force. In between the onset of chaos and band merging crisis a periodic window region occurs. Fig. 7 shows the plot of  $x_n$  versus n where n is the time t in steps of  $2\pi/\omega$  for three values of f. Intermittent dynamics is clearly seen in Figs. 7(a) and 7(b).

**Table 1** Summary of bifurcation phenomena of the classical Morse oscillator (Eq. 9) in the presence of different shape of periodic forces for d = 0.8,  $\beta$  = 8.0,  $\alpha$  = 1 and  $\omega$  = 2.0.

	Critical values of amplitude of the various forces					
Bifurcations	Sine wave	Square Wave	Rectified	Symmetric	Asymmetric	Modulus
			sine	saw-tooth	saw-tooth	of sine
			wave	wave	wave	wave
Transcritical	1.60794	1.31984	1.62150	1.99083	2.92987	1.20529
Period-2T	2.13431	1.66650	2.13161	2.72833	4.54104	2.38566
Period-4T	2.37859	1.71744	2.37279	3.02356	5.09425	2.50147
Period-8T	2.44005	1.77265	2.43652	3.08795	5.23061	2.50563
Period-16T	2.45117	1.72875	2.45601	3.12257	5.26118	2.50893
Onset of	2.45558	1.73151	2.45920	3.13335	5.28020	2.50922
chaos						
Intermittency	2.57625	1.81901	2.51847	3.27167	5.35725	2.51068

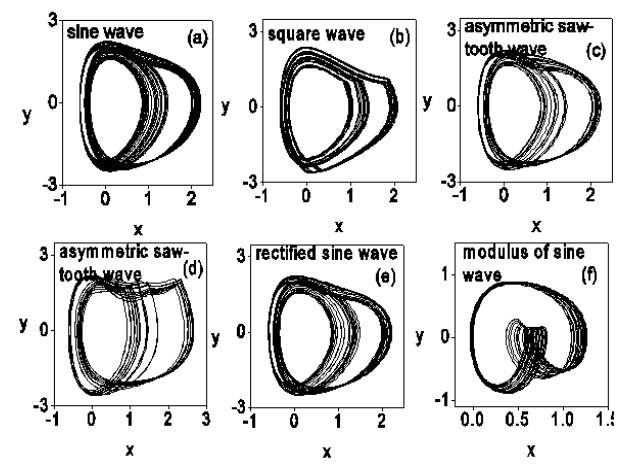


**Fig. 4** Phase portraits of the system (Eq. 9) at the accumulation of period doubling phenomenon (onset of chaos) for various forces. The values of other parameters are d=0.8,  $\beta=8.0$ ,  $\alpha=1$  and  $\omega=2$ .

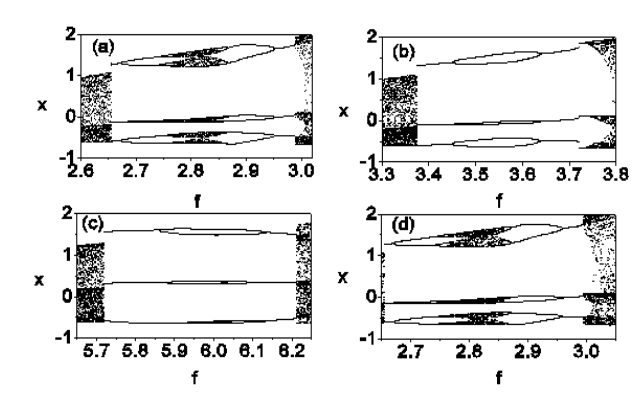
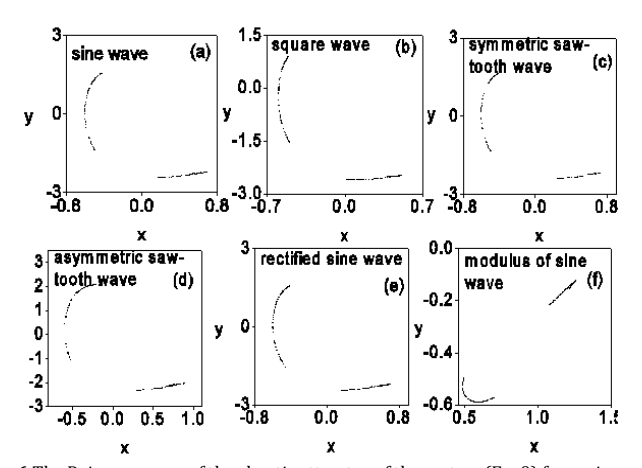
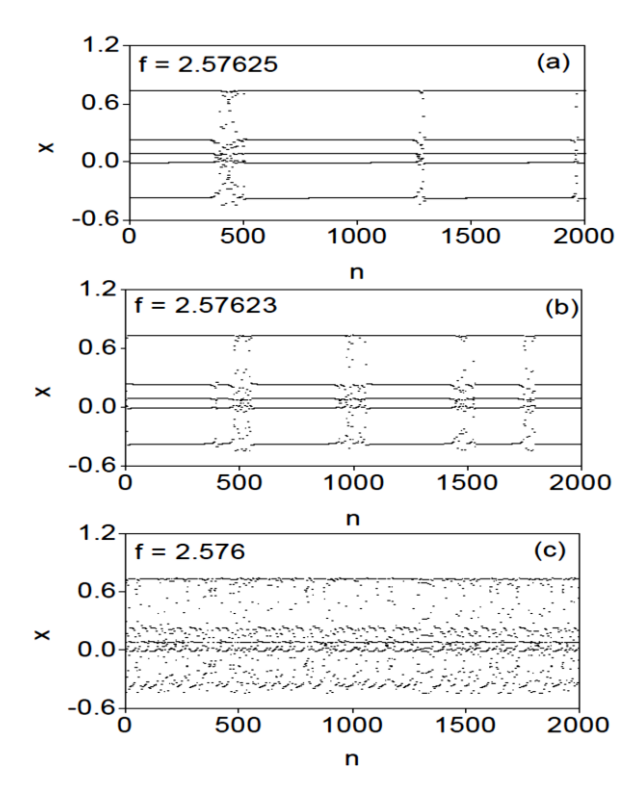


Fig. 5 Bifurcation structures of the sysyem (Eq. 9) for showing the period-3 bubble orbit . The values of other parameters are d=0.8,  $\beta=8.0$ ,  $\alpha=1$  and  $\omega=2$ .



**Fig. 6** The Poincare maps of the chaotic attractor of the system (Eq. 9) for various forces. The values of other parameters are d=0.8,  $\beta=8.0$ ,  $\alpha=1$  and  $\omega=2$ .



**Fig. 7**  $x_n$  versus n of the system (Eq. 9) driven by periodic sine wave force ( where n is the time t in steps of  $2\pi/\omega$ ) for three values of f. Intermittent dynamics is clearly seen in figs.7(a) and 7(b).

In these figures, the laminar region with the unstable period-5T orbit interrupted by chaotic burst is observed. This type of behaviour is observed for other forces in system (Eq. 9). However the period of the laminar region is found to be different for other forces. For force such as square wave, symmetric saw tooth wave, rectified sine wave the period of the orbit in the laminar region is 5T while for the forces namely asymmetric saw tooth wave and modulus of sine wave the period is 6T.

## 3.4 Bifurcation Patterns for $\omega$ = 0.5

So far we studied the response of the system with  $\omega=2.0$ , the dynamics of the system (Eq. 9) is analysed for several values of  $\omega$ . As an example, Fig. 8 presents the result for  $\omega=0.5$ .

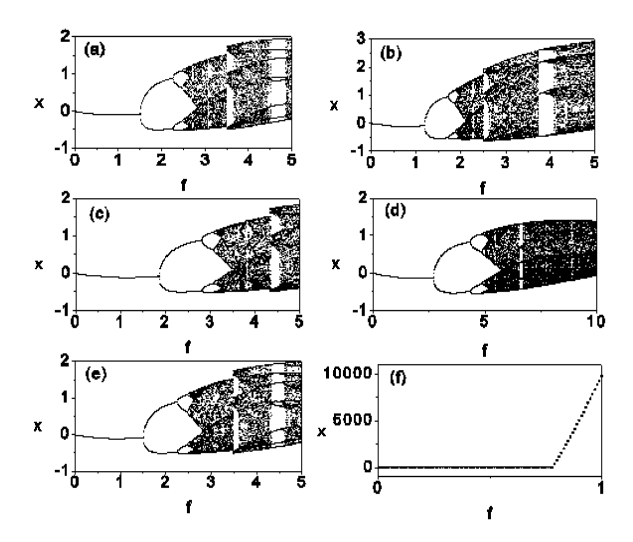


**Fig. 8** Bifurcation structures for the system (Eq. 9) driven by various forces (a) sine wave (b) square wave (c) symmetric saw-tooth wave (d) asymmetric saw-tooth wave (e) rectified sine wave and (f) modulus of sine wave. The other parameters values are d=0.8,  $\beta=8.0$ ,  $\alpha=1$  and  $\omega=0.5$ .

Here again we can clearly notice many similarities and differences in the bifurcation phenomenon when the parameter f is varied. For sine wave force at f =1.51282 period-2 bifurcation occurs at which maximal Lyapunov exponent  $\lambda_m \approx 0$ . When the sine wave force is replaced by other

forces similar behaviour is found except modulus of sine wave force. Only period-*T* orbit is observed in this force. Period-2 bifurcation observed are  $f_{\text{sq}} = 1.24823$ ,  $f_{\text{sst}} = 1.89512$ ,  $f_{\text{ast}} = 2.58175$  and  $f_{\text{rsw}} = 1.50383$ . That is this bifurcation occurs relatively earlier in the case of square wave whereas it is very much delayed by the asymmetric saw tooth wave force. The period doubling sequence accumulated at f = 2.75621 for sine wave force. At this value of f onset of chaos is observed. For other forces  $f_{sq} = 2.0542$ ,  $f_{sst} =$ 3.25621,  $f_{ast} = 5.27452$  and  $f_{rsi} = 2.52932$ . Chaotic motion is not observed in modulus of sine wave force. (Fig. 8f). For  $\omega$  = 0.5, period-3 bubble orbit is not observed in system (Eq. 9) for all the forces but it is observed for  $\omega$  = 2.0 in all forces except square wave and modulus of sine wave force. The bifurcation structures for the system (Eq. 9) driven by periodic sine wave force in  $(\omega, x)$  plane for four values of f namely, f = 1.0, 2.5, 3.5, 5.0 are plotted in Fig. 9. The effect of f can be clearly seen in the bifurcation diagrams Figs. 9(a-d). For f = 1.0, the system (Eq. 9) driven by  $f \sin \omega t$  shows completely periodic behaviour (Fig. 9a). When f is increased from the value 1, the system (Eq. 9) undergoes reverse period-doubling bifurcation, periodic windows, chaos etc. which is presented in Fig. 9(b-d). When the force  $f\sin\omega t$  is replaced by other forces similar behaviour is found to occur.

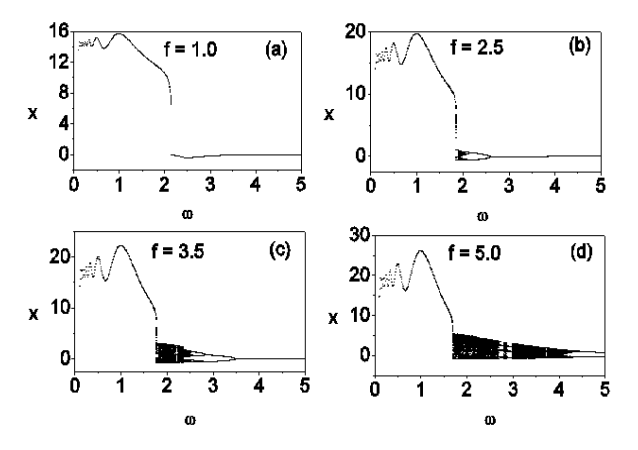


**Fig. 9** Bifurcation structures for the system (Eq. 9) driven by periodic sine wave force in  $(\omega, x)$  plane for four values of f. The other parameters are d = 0.8,  $\alpha$  = 1.0 and  $\beta$  = 8.0

## 4. Conclusion

In this paper, we numerically studied the bifurcation structures of classical Morse oscillator driven by various periodic forces. The various bifurcation diagrams clearly show that the system (Eq. 1) exhibits qualitative changes at the critical values of the control parameters as they are varied smoothly. For a particular set of parameter values we have shown the occurrence of various bifurcations of chaos, routes to chaos, period-3 bubble orbit, reverse-period doubling bifurcation and noticed many similarities and differences in the bifurcation structures in the presence of various periodic forces. We compared the effect of forces on transcritical bifurcation, period doubling phenomenon, onset of chaos etc. for a particular set of the parameters. It is important to study the effect of other types of forces such as amplitude modulated wave and frequency modulated wave. Melnikov analytical technique can be employed to Eq. 1 to investigate onset of horseshoe chaos.

#### References

- P.M. Morse, Diatomic molecules according to wave mechanics II, vibrational levels, Phys. Rev. 34 (1929) 57-64.
- [2] G. Herzberg, Spectra of diatomic molecules, Van Nortrand, New York, 1950.
- [3] P.M. Morse, H. Feshbach, Methods of theoretical physics parts 1 and 2, Mc Graw-Hill Book Co., New York, 1953.
- [4] J. Guckenheimer, P. Holmes, Nonlinear oscillations, Dynamical systems and Bifurcations of vector fields, Springer-Verlag, New York, 1983.
- [5] M. Lakshmanan, S. Rajasekar, Nonlinear dynamics, Integrability, Chaos and Patterns, Berlin, Springer, 2002.
- [6] S.K. Grap, Classical aspects of laser excitation of a Morse oscillator, J. Chem. Phys. 75(1) (1983) 67-78.
- [7] R.C. Brown, R.E. Wyatt, Quantum mechanical manifestation of Cantori, Wave packet localization in stochastic region, Phys. Rev. Lett. 51 (1986) 1-6.
- [8] R.B. Walker, R.K. Preston, Quantum versus classical dynamics in the treatment of multiphotons excitation of the anharmonic oscillator, J. Chem. Phys. 67 (1977) 2017-2028
- [9] G.D. Billing, G. Jolicard, The linearly forced Morse Oscillator, Chem. Phys. Lett. 102(6) (1983) 491-500.
- [10] D.S. Ray, Quantum Statistical theory of damped driven Morse oscillator: Bistable features and spectral characteristics, J. Chem. Phys. 92 (1990) 1145-1152.
- [11] R.M.O. Galvao, L.C.M. Miranda, J.T. Mendonca, Stochastic dissociation of a laser driven Morse oscillator, J. Phys. B; At. Mol. Phys. 17 (1984) L577-L582.
- [12] M. Tung, J.M. Yuan, Dissipative quantum dynamics: Driven molecular vibrations, Phys. Rev. A 36 (1987) 4463-4470.
- [13] G.C. Lie, J.M. Yuan, Bistable and chaotic behaviour in a damped driven Morse oscillator. A classical approach, J. Chem. Phys. 84 (1986) 5486-5493.
- [14] W. Knob, W. Lauterborn, Bifurcation structure of the classical Morse oscillator, J. Chem. Phys. 93(6) (1990) 3950-3957.
- [15] S. Parthasarathy, M. Lakshmanan, Analytic structure of the damped driven Morse oscillator, Phys. Lett. A 157(6) (1991) 365-370.
- [16] G. Rong-Wei, H. De-Bin, Z. Li-Zhen, Dynamical behaviour of the driven Morse oscillator, Jour. Shangai Univ. 7(4) (2003) 340-342.
- [17] Z. Jing, J. Deng, J. Yang, Bifurcations of periodic orbits of chaos in damped and driven Morse oscillator, Chaos, Soliton. Fractals 35 (2008) 486-505.
- [18] J. Heagy, J.M. Yuan, Dynamics of an impulsively driven Morse oscillator, Phys. Rev. A 41(2) (1990) 577-581.
- [19] S. Behnia, A. Akhshani, M. Panahi, R. Asadi, Controlling chaos in damped and driven Morse oscillator via slave-master feedback, Acta Physica Polonica A 123 (2013) 7-12.
- [20] C. Gan, Q. Wang, M. Perc, Torus breakdown and noise induced dynamics in the randomly driven Morse oscillator, J. Phys. A: Math. Theor. 43 (2010) 125102.
- [21] R. Kapral, M. Schell, S. Fraser, Chaos and fluctuations in nonlinear dissipative systems, J. Phys. Chem. 86(12) (1982) 2205-2217.
- [22] D. Beigie, S. Wiggins, Dynamics associated with a quasi-periodically forced Morse oscillator: Application to molecular dissociation, Phys. Rev. A 45(7) (1992) 4803-4827,
- [23] L. Zhou, F. Chen, Chaotic motions of a damped and driven Morse oscillator, Appl. Mech. Mat. 459 (2014) 505-510.
- [24] K. Abirami, S. Rajasekar, M.A.F. Sanjuan, Vibrational resonance in the Morse oscillator, Pram. J. Phy. 81(1) (2013) 127-141.
- [25] K.M. Christoffel, J.M. Bowman, Classical trajectory studies of multi photon and overtone absorption of hydrogen fluoride contents, J. Phys. Chem. 85(15) (1981) 2159-2163.
- [26] P.S. Dardi, S.K. Gray, Classical and Quantum mechanical studies of HF in an intense laser field, J. Chem. Phys. 77(3) (1982) 1345-1353.
- [27] M.E. Goggin, P.W. Milonni, Driven Morse oscillator: Classical Chaos, quantum theory and Photo dissociation, Phys. Rev. A 37 (1988) 796-806.
- [28] J.R. Ackerhalf, P.W. Milonni, Chaos and incoherence in a model of multiplephoton excitation of molecular vibrations, Phys. Rev. A 34(2) (1986) 1211-1221.
- [29] A. Memboeuf, K.S. Aubry, Targeted energy transfer between a Rotor and a Morse oscillator: A model for selective chemical dissociation, Physica D 207 (2005) 1-23.